Multiparametric Magnetic Resonance Imaging Allows Non-Invasive Functional and Structural Evaluation of Diabetic Kidney Disease

Kianoush Makvandi,[1] Paul D. Hockings,[2,6] Gert Jensen,[1] Tim Unnerstall,[3] Henrik Leonhardt,[3] Lisa V. Jarl,[2] Camilla Englund,[2] Susan Francis,[4] Anna K. Sundgren,[5] Johannes Hulthe,[2] Seema Baid-Agrawal[1,7]

[1]Department of Molecular and Clinical Medicine/Nephrology, The Institute of Medicine, Sahlgrenska Academy, University of Gothenburg, Sweden
[2]Antaros Medical, Molndal, Sweden
[3]Department of Radiology, Sahlgrenska University Hospital, Gothenburg, Sweden
[4]Sir Peter Mansfield Imaging Centre, University of Nottingham, Nottingham, UK
[5]Late-Stage Development, Cardiovascular, Renal and Metabolism (CVRM), BioPharmaceuticals R&D, AstraZeneca, Gaithersburg, MD, USA
[6]MedTech West, Chalmers University of Technology, Gothenburg, Sweden
[7]Transplant Center, Sahlgrenska University Hospital, Gothenburg, Sweden

Correspondence to: Seema Baid-Agrawal; E-mail: seema.baid-agrawal@vgregion.se

GRAPHICAL ABSTRACT

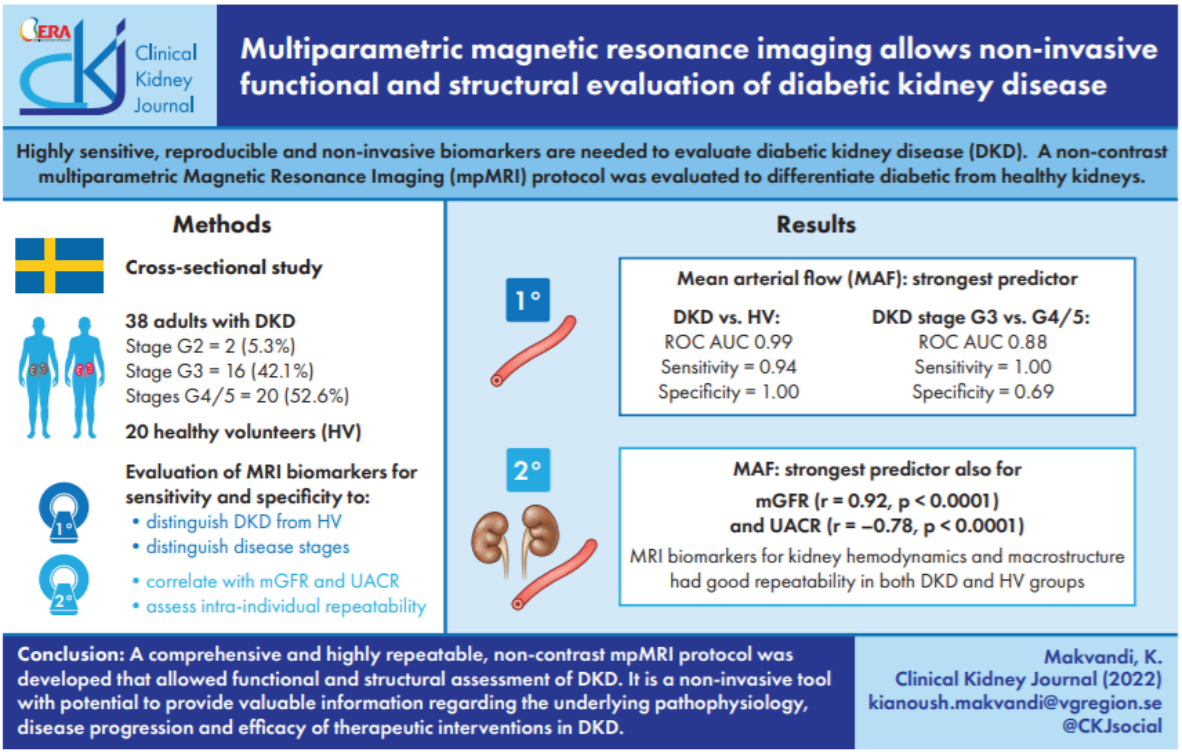

ABSTRACT

Background. We sought to develop a novel non-contrast multi-parametric MRI (mpMRI) protocol employing several complementary techniques in a single scan session for a comprehensive functional and structural evaluation of diabetic kidney disease (DKD).

Methods. In the cross-sectional part of this prospective observational study, 38 subjects aged 18–79 years with type 2 diabetes and DKD (estimated glomerular filtration rate [eGFR] 15–60 ml/min/1.73 m^2), and 20 age- and gender-matched healthy volunteers (HV) underwent mpMRI. Repeat mpMRI was performed in 23 DKD subjects and 10 HV. By measured GFR (mGFR), 2 DKD subjects had GFR stage G2, 16 stage G3, and 20 stage G4/5. A wide range of MRI-biomarkers associated with kidney hemodynamics, oxygenation, and macro/micro-structure

were evaluated. Their optimal sensitivity, specificity and repeatability to differentiate diabetic versus healthy kidneys, and categorize various stages of disease as well as their correlation with mGFR/albuminuria was assessed.

Results. Several MRI-biomarkers differentiated diabetic from healthy kidneys and distinct GFR stages (G3 versus G4/5); mean arterial flow (MAF) was the strongest predictor (sensitivity=0.94 and 1.0, specificity=1.00 and 0.69, p=0.04 and 0.004, respectively). Parameters significantly correlating with mGFR were specific measures of kidney hemodynamics, oxygenation, microstructure and macrostructure, with MAF being the strongest univariate predictor (r=0.92, p<0.0001).

Conclusions. A comprehensive and repeatable non-contrast mpMRI protocol was developed that as a single, non-invasive tool allows functional and structural assessment of DKD, which has the potential to provide valuable insights into underlying pathophysiology, disease progression and analysis of efficacy/mode of action of therapeutic interventions in DKD.

Keywords: biomarkers, chronic kidney disease, diabetic kidney disease, magnetic resonance imaging (MRI), multiparametric, type 2 diabetes

INTRODUCTION

Chronic kidney disease (CKD) associated with diabetes mellitus (DM), named diabetic kidney disease (DKD), occurs in approximately 30-40% of patients with type 2 DM (T2DM) (1, 2). DKD is associated with increased morbidity and mortality, and the leading cause of kidney failure (ESKD) worldwide (1, 2). With increasing prevalence of T2DM, the global DKD burden is expected to rise (1, 2). To prevent ESKD, early identification of patients at high risk of DKD progression enabling timely treatment is important. However, predicting the evolution of DKD remains difficult due to its highly variable progression, particularly in T2DM (1).

Established kidney biomarkers, such as estimated glomerular filtration rate (eGFR) or proteinuria, provide only a rough estimation of overall kidney damage (3). Measured GFR (mGFR), using plasma clearance of filtration markers, more accurately measures kidney function than eGFR, but is time-consuming and cumbersome for screening and ambulatory care (4). Moreover, as the kidney can partially compensate for lost function, significant kidney fibrosis may occur without a measurable change in GFR (5). As regards proteinuria, intra-individual variations are considerable (6). Thus, these routinely used biomarkers neither provide insights into underlying DKD pathophysiology and degree of anatomical damage nor allow risk stratification (7, 8). Various DKD phenotypes are well-recognized and other pathways to ESKD independent of albuminuria have been postulated suggesting different pathophysiology not readily detected by conventional biomarkers (9). Whilst kidney biopsy is essential for assessing kidney pathophysiology in DKD (10), it is not suitable for long-term, serial monitoring of dynamic process of disease progression or response to therapy due to its invasive nature, an increased risk of bleeding in

uremic patients (11) and susceptibility to sampling errors. Therefore, kidney biopsy is not routinely performed in clinical practice for DKD diagnosis or monitoring (12). There is a clear need for new, sensitive, reproducible and non-invasive biomarkers to enhance our understanding of DKD pathophysiology, progression and efficacy/modes of action of therapeutic interventions in clinical practice/trials.

Novel, non-contrast magnetic resonance imaging (MRI) techniques are potential methods to non-invasively assess and quantify functional and pathophysiological changes in CKD (13-17). Employing such complementary MRI techniques simultaneously in multiparametric Magnetic Resonance Imaging (mpMRI) may provide more comprehensive information across individual kidney compartments on microstructure (including kidney fibrosis and inflammation), macrostructure (kidney volume), oxygenation, and hemodynamic measurements of renal artery blood flow and perfusion (13, 18).

In a cross-sectional study using mpMRI in CKD patients (excluding DKD), several MRI-biomarkers correlated with albuminuria, eGFR and histopathological measures of interstitial fibrosis (19). Nevertheless, more studies identifying the most appropriate MRI-biomarkers of kidney function and structure, and their technical and clinical validation are required before mpMRI can be adopted in clinical practice (14, 19). To our knowledge, no study has specifically investigated mpMRI in DKD, although individual MRI techniques have been evaluated to detect early changes and renal blood flow in DKD (20-23).

In this kidney mpMRI study, we evaluated a range of MRI-biomarkers for their optimal sensitivity and specificity in distinguishing DKD subjects from healthy volunteers (HV), and between different disease stages. Secondary aims were to:
(i) analyze intra-individual repeatability of MRI-biomarkers to capture natural biological variability;
(ii) assess correlation of each MRI-biomarker to conventional biomarkers of kidney function and damage (i.e., mGFR, Urine Albumin-to-Creatinine Ratio, UACR); and
(iii) develop a bifactorial model to predict mGFR using MRI-biomarkers.

MATERIALS AND METHODS

Study Design and Participants

This cross-sectional and longitudinal observational investigator-driven single-center study conducted at Sahlgrenska University Hospital (SU), Gothenburg, Sweden was approved by the Regional Ethics Review Board and carried out according to the Helsinki Declaration of 1975 (revised 2013). Subjects with T2DM and DKD, and HV were enrolled during the same period after obtaining written informed consent from all subjects.

DKD subjects: Between 11/2016-6/2018, 48 subjects with T2DM and DKD from the outpatient clinics of the Nephrology Department at SU/affiliated hospitals (n=25), and primary care clinics in Gothenburg (n=23) were screened by reviewing medical records (Figure 1). Eligible subjects with T2DM and DKD were identified by medical history, UACR and eGFR using the CKD-EPI (CKD Epidemiology Collaboration) creatinine equation (24) within last three months of screening. The diagnosis of DKD was per treating physician's assessment. The inclusion/exclusion criteria are stated

in Table 1. DKD subjects were stratified by mGFR into four GFR stages (G2–G5) as per the Kidney Disease Improving Global Outcomes (KDIGO) classification of CKD (25).

Control group (HV): Twenty-five age (±5 years)- and gender-matched HV were screened and recruited by the Clinical Trial Center of the SU via local advertisement, as per the inclusion/exclusion criteria in Table 1.

Clinical/Laboratory Assessments

Demographic data, medical history, physical examination (including body mass index [BMI]), blood samples and first-morning urine sample for determination of UACR were collected at baseline visit. The mGFR was evaluated using the iohexol clearance test as described in **Supplementary Methods** (26).

Kidney mpMRI Examination

All subjects underwent a kidney mpMRI examination within 3 weeks following mGFR assessment; 33 subjects (10 HV, 23 DKD subjects) underwent a second MRI examination 2–3 weeks (maximum 6 weeks) after the first MRI examination. Subjects drank 250 ml of water before the MRI scan. The MRI examination was performed on a Philips Achieva dStream 3T (Philips Healthcare, Best, Netherlands) without any contrast agents with total scan time of 50 minutes. MRI-biomarkers associated with kidney hemodynamics, oxygenation, and macro- and micro-structure were evaluated (Table 2) using the image acquisition/analysis protocols described in **Supplementary Methods**.

Statistical Analysis

The ability of each MRI biomarker to discriminate between the DKD and HV groups was evaluated using univariate logistic regression analysis with the DKD and HV groups as a dependent variable and the MRI biomarker as an independent variable. The assessment of discrimination of the fitted logistic regression model was done via the receiver operating characteristic (ROC) curve and the area under the ROC curve (ROC AUC). The Youden cut-off and its sensitivity and specificity were calculated (27). The same logistic regression methods and analyses were used to assess discrimination between stages G3 and G4/5.

The intra-individual repeatability of the MRI-biomarkers was assessed using the intra-individual coefficient of variance (CV) and the intra-class correlation coefficient (ICC) type (2,1) based on the values from the repeated MRI measurements (28). Each MRI biomarker's linear association with mGFR and UACR was evaluated using univariate linear regression with mGFR or UACR as a dependent variable and MRI biomarker as an independent variable. The Pearson correlation with mGFR and the Spearman correlation with UACR was calculated to evaluate the association with each MRI biomarker.

Bivariate MRI predictors of mGFR were evaluated using a pre-defined approach; each pair of the MRI predictors with a P-value <0.10 in the univariate linear regression analysis was entered into a stepwise linear regression model. A significance level of 0.05 in model improvement was required to allow variables into the model. Because reduced GFR is known to correlate with increased UACR (29), bivariate predictors of UACR were examined using mGFR as one variable and

adding one MRI endpoint using linear regression in the DKD subjects. The HV were excluded from this analysis as they had no significant UACR values. Continuous data are expressed using mean (standard deviation) or median (interquartile range) and categorical data as numbers (percentages). Two-sided P-values <0.05 were considered significant. Statistical analyses were done using SAS© v9.4 software. Sample size calculation is described in **Supplementary Methods**.

RESULTS

As in Figure 1, 44/48 screened DKD subjects were found to be eligible. Of these, two classified as stage G3 and G4 by eGFR at screening were found by mGFR to have stage G2 (mGFR 62 and 64 mL/min/1.73m^2) and G5 (mGFR 11 and 12 mL/min/1.73m^2), resulting in 42 subjects in stages G3–G5. Twenty-three subjects underwent two MRI scans, 16 one scan, and the remaining five could not complete MRI due to claustrophobia. Total 39 subjects completed the study (N=2 stage G2, N=37 stages G3–G5), of whom one stage G4 subject was excluded due to a revised diagnosis of hydronephrosis as a contributory cause of CKD, based on the MRI finding and past history. Thus, the analysis set included 38 DKD subjects (stages G2–G5) for correlation analysis and 36 for group comparisons (16 in stages G3 versus 20 in G4/G5) (Figure 1). Of the 25 screened HV, 20 met the inclusion criteria and were included in the analysis set. Of these, 10 underwent two MRI scans (Figure 1).

As regards the demographic and baseline clinical characteristics (Table 3), the main differences between DKD subjects and HV were in the proportion of males (83%

versus 75%), systolic blood pressure (150 mmHg versus 133 mmHg) and BMI (27.9 versus 25.5 kg/m^2).

Differentiation Between HV and DKD Subjects with MRI-biomarkers

Anatomical T_1-weighted MR images showed clear corticomedullary contrast in HV, reduced contrast in stage G3 subjects, and virtually no contrast in the stage G4/5 subjects (example shown in Figure 2). Representative mpMRI images are shown in Figure 3. Examples of renal blood flow velocity profiles are shown in Figure 4.

The strongest predictive properties differentiating HV and DKD subjects were hemodynamic MRI-biomarkers (MAF, end diastolic velocity, RARI, ASL perfusion cortex, and global perfusion) with sensitivity and specificity for cut-off values of 0.81–0.94 and 0.90–1.00, respectively (Table 4). The strongest predictor was MAF with a Youden cut-off value of 803 ml/min/1.73 m^2, sensitivity of 0.94 and specificity of 1.00 (Table 3, Figure 5).

HV and DKD subjects could also be distinguished using MRI-biomarkers of kidney microstructure (R_1 cortex, ADC cortex and medulla, and IVIM Slow Diffusion cortex and medulla), macrostructure (kidney volume), and oxygenation in the medulla assessed with BOLD R_2* (Table 4). Moreover, BOLD R_2* values were higher in the medulla versus cortex in both HV (cortex: 17.3±1.4/s, medulla: 26.0±2.3/s) and DKD subjects (cortex: 17.1±1.4/s medulla: 23.5±3.7/s), indicative of lower oxygenation in the medulla than the cortex (Table 4).

Differentiation Between Stages G3 and G4/5 in DKD Subjects with MRI-Biomarkers

The strongest predictive properties to differentiate between stages G3 and G4/5 were also hemodynamic MRI-biomarkers– MAF, peak systolic velocity, end-diastolic velocity and global perfusion measurements all showed a ROC AUC >0.75 (Table 5), the best predictor again being MAF (Figure 6). Youden cut-off values for separating the two groups were 605 ml/min/1.73 m^2 for MAF, 53.2 cm/s for peak systolic velocity, 8.35 cm/s for end-diastolic velocity, with sensitivities and specificities of 0.90–1.00 and 0.69–0.81, respectively (Table 5). MRI-biomarkers for kidney microstructure also enabled stage G3 to be distinguished from G4/5, where R_1 in the cortex showed the highest predictive properties (ROC AUC=0.76) (Table 5).

The eGFR also showed strong predictive properties for distinguishing between stages G3 and G4/5, with high sensitivity and specificity, whereas the UACR showed a lower ROC AUC (0.72), with sensitivity=0.45 and specificity=0.94 for the cut-off value of 97 mg/mmol (Table 5).

MRI-Biomarker Repeatability in HV and DKD Subjects

Intra-individual CV values were lowest for RARI (2%), R_1 in cortex and medulla (2%), and for cortical and medullary BOLD R_2* (≤5%) suggesting good repeatability. The CV values ranged between 2–12% for all MRI-biomarkers except ASL perfusion cortex (CV=33%), and IVIM Fast Diffusion and Perfusion Fraction measurements (CV>25%) (Table 6). The ICC values were ≥89% for MAF, peak systolic velocity, end-diastolic velocity, RARI, global perfusion, cortical R_1, medullary BOLD R_2*, and kidney volume (Table 6).

Correlation of MRI-Biomarkers with mGFR and UACR

MRI-biomarkers with strong predictive properties distinguishing both HV and DKD subjects and GFR stages were also strongly correlated to mGFR, the reference measurement. There were statistically significant correlations (P<0.05) between mGFR and MRI-biomarkers: kidney hemodynamics (MAF, end-diastolic and peak systolic velocity, RARI, cortical and global perfusion), kidney microstructure [cortical and medullary ADC, IVIM Slow Diffusion (D) in cortex and medulla, cortical R_1], oxygenation (medullary BOLD R_2*) and macrostructure (kidney volume). The mGFR correlation to RARI was negative indicating an increase in renal arterial resistance with kidney function decline (Table 7).

The strongest univariate MRI predictor of mGFR was MAF (r=0.92, p<0.0001) (Figure 7). A slight improvement in the prediction occurred when combining MAF with ASL perfusion cortex, RARI, ADC cortex, R_2* medulla, D or R_1 cortex (r=0.92-0.93), where all measurements with a P-value <0.05 were included in the model.

Univariate analysis showed that several MRI-biomarkers correlated significantly with UACR (Table 7). However, UACR correlated negatively with mGFR (Spearman correlation coefficient -0.81, p<0.0001). Bivariate prediction of UACR using linear regression with mGFR as one variable and adding one MRI endpoint showed that only R_1 cortex, R_1 medulla, D cortex, and IVIM Perfusion Fraction (f) cortex significantly improved prediction of UACR (Table 7). Many other parameters that initially correlated with UACR in the univariate analysis were no longer significant in the bivariate analysis (Table 7). In particular, hemodynamic parameters and kidney volume appeared to be linked to UACR via their effect on mGFR.

DISCUSSION

This is the first study, to our knowledge, evaluating the optimal sensitivity and specificity of an array of MRI-biomarkers using mpMRI in DKD, as opposed to a mixed CKD group (19, 30) and demonstrating intra-individual repeatability within DKD. Importantly, a robust, non-contrast mpMRI protocol was developed that allowed comprehensive evaluation of kidney hemodynamics, micro- and macro-structure, and oxygenation, and as a single, non-invasive tool distinguished HV from DKD, and various GFR stages (G3 versus G4/5). Several MRI-biomarkers correlated strongly with mGFR and/or UACR indicating that their biological relevance while providing additional information on underlying pathophysiology.

MRI-biomarkers with the strongest predictive properties to differentiate HV from DKD subjects were specific for kidney hemodynamics, particularly MAF, RARI and end-diastolic velocity. In accordance with disease pathophysiology, MAF was lower in DKD subjects than HV. Global perfusion and ASL measure kidney perfusion; both showed highly significant decreases in DKD subjects versus HV, as expected. Global perfusion, however, was greater than that reported by Buchanan *et al*.(19) in a non-diabetic CKD population, which may be explained by the fact that they calculated global perfusion using whole kidney volume rather than kidney parenchymal volume. Likewise, MRI-biomarkers associated with kidney macrostructure (e.g., kidney volume) and microstructure (e.g., R_1 and ADC in cortex, and R_2* in medulla) were able to differentiate HV from DKD subjects. Not surprisingly, we found a significant decrease in parenchyma volume in DKD subjects versus HV. Hemodynamic MRI-biomarkers were also able to distinguish between

stages G3 and G4/5, particularly MAF, peak systolic velocity, end-diastolic velocity and global perfusion, as was the microstructure MRI-biomarker R_1.

As far as we are aware, the hemodynamic MRI-biomarkers end diastolic velocity, peak systolic velocity and RARI have only been evaluated in renal arteries of healthy individuals (31). In this study, end diastolic velocity and RARI enabled HV to be differentiated from DKD subjects, and both end diastolic velocity and peak systolic velocity could distinguish DKD subjects with stage G3 versus stage G4/5. These are novel MRI-biomarkers that may provide additional insights into DKD pathophysiology.

Some MRI-biomarkers were not found to be directly related to kidney function, including IVIM parameters [Fast Diffusion (D*), Perfusion Fraction (f)] and the Magnetization Transfer Ratio (MTR). The latter was reasonably repeatable, thereby showing potential for clinical trials; however, its correlation coefficient to mGFR was poor and it showed no significant correlations to other MRI, plasma, or urine biomarkers when corrected for multiple comparisons. There are mixed positive (32) and negative (33) reports regarding MTR correlation with kidney fibrosis in animal models. The D* and f IVIM MRI measures were the least repeatable and may reflect kidney perfusion fluctuations during the cardiac cycle, and similar variability in these parameters has been demonstrated (34, 35). Their inability to predict CKD may reflect a lack of precision *per se* as opposed to being unimportant for underlying biology.

Most MRI-biomarkers in our HV group were similar to those reported previously (Table 8) with some differences. In our HV, MAF was slightly lower than that reported for a healthy population (36), although our subjects were 67 ± 6 years old and blood flow is expected to decrease with age. Others have even reported much lower values in healthy individuals (34). Our kidney macrostructure evaluation in HV shows a total parenchyma for both kidneys slightly smaller than whole kidney volume reported in live kidney donors using Computer Tomography (CT) (37) and that of the total cortical volume in another CT study (38). The slightly smaller volume may be due to older HV age compared to kidney donors in the aforementioned study (37), and well-known reduction in kidney size with age (39). Moreover, we measured parenchyma volume, not total kidney volume. Overall, these data are consistent with previous studies in healthy populations and confirm our MRI protocol validity.

We also tested the intra-individual repeatability of MRI-biomarkers in both groups to evaluate them as monitoring biomarkers. Hemodynamic and kidney macrostructure measures (specifically R_1 and ADC in cortex, and R_2* in medulla) had good repeatability, while ASL was less repeatable. This is the first study to demonstrate intra-individual repeatability of a mpMRI protocol in DKD, suggesting that these MRI-biomarkers are well-suited for clinical trials.

Some MRI-biomarkers correlated with established biochemical surrogate biomarkers of kidney function and damage, namely GFR and UACR (40). The GFR is the volume of fluid filtered from glomeruli, representing plasma flow from the glomerulus into Bowman's space. The tight coupling between MAF and mGFR in our study is therefore predictable (41) albeit greater than that found in a mixed CKD population

(19), and reflects the precision of this imaging technique. Indeed, strong correlation between MAF and mGFR made it difficult to meaningfully improve mGFR prediction by adding an independent imaging predictor in a bivariable model. Both global perfusion and ASL also highly correlated with mGFR, although intra-individual repeatability for global perfusion was much better than for ASL. The purpose of this work is not to replace readily available GFR measurement routines with an expensive imaging technique but to provide additional mechanistic data that may be useful to understand the pathophysiology of the underlying disease as well as efficacy/mechanisms of action of novel drugs.

End diastolic velocity, RARI and cortical R_1 also correlated with mGFR here, such that end diastolic velocity decreased and RARI (resistance) increased with declining kidney function. RARI measured with doppler ultrasound increases with and is an independent risk factor for worsening kidney function in both CKD and DKD (42-44). The sodium glucose cotransporter 2 inhibitor (SGLT2i) dapaglifozin significantly reduces RARI measured by ultrasound in individuals with T2DM (45). Given the good repeatability of end diastolic velocity and RARI here, these MRI-biomarkers may find application in clinical trials of novel therapies designed to reduce kidney fibrosis and subsequent renal arterial resistance.

Several MRI-biomarkers, including MAF and cortical R_1, correlated significantly with UACR. Buchanan *et al*. (19) also saw significant correlations between cortical T_1 (T_1=1/R_1), MAF, and several other MRI-biomarkers with log Urine Protein-to-Creatinine Ratio (UPCR). Since UACR or UPCR correlated with mGFR in both their (19) and our study, we checked if a bivariate model of UACR combining an MRI

measure with mGFR could statistically improve UACR prediction compared to mGFR alone. Only R_1 (both cortical and medullary) and cortical IVIM D and f values remained significant UACR predictors. Thus, they may be valuable tools to understand and monitor kidney damage beyond the decline in kidney function as DKD progresses.

Blood flow and oxygen levels in the kidney cortex and medulla are seriously impaired in moderate-to-severe kidney disease (46) and kidney tissue hypoxia is regarded as the common pathway for all CKD. Since renal blood flow influences both oxygen supply and demand, evaluating oxygen levels independently of perfusion is essential (47). BOLD-MRI is the only non-invasive method to measure kidney oxygen levels, and a high kidney cortical R_2* (corresponding to low oxygenation) by BOLD-MRI was shown to predict poor outcomes in some studies (15, 48, 49). In our study, using mpMRI, cortical R_2* did not correlate with GFR or UACR, in line with some other studies (19, 50). Some of the MRI-biomarkers may be more suitable as prognostic biomarkers, however, due to the cross-sectional nature of this part of our study, we were unable to explore any prognostic correlation.

Our study has several strengths. A comprehensive, non-contrast mpMRI protocol allowed investigation of multiple aspects of kidney function and structure in a single 50-minute sitting. A well-characterized population of individuals with T2DM and DKD, and HV were included. Standardized hydration protocol before MRI ensured uniform hydration in all. Additionally, mGFR enabled accurate evaluation of kidney function. Finally, repeat MRI in half of the subjects allowed evaluation of MRI biomarkers' repeatability. Limitations include lack of histologic "gold standard" to validate MRI

findings, lack of generalizability to non-Swedish populations, and inclusion of DKD subjects based only on a clinical diagnosis. Thus, some subjects may have had DKD together with hypertensive nephrosclerosis due to coexisting hypertension, as often occurs in a real-world setting. We also want to point out that in the absence of a non-diabetic CKD population, our findings may not be specific for DKD but may represent CKD in general.

In conclusion, for the first time a comprehensive and robust non-contrast mpMRI protocol was developed that allows non-invasive functional and structural evaluation of DKD. This novel approach has potential to provide valuable insights into underlying pathophysiology, disease progression and analysis of efficacy/mode of action of therapeutic interventions in DKD, and therewith improve management and prognosis of these patients. Studies assessing the influence of interventions such as SGLT2i and renin-angiotensin-aldosterone system blockers on MRI biomarkers are currently underway. The ongoing longitudinal part of our study will explore prognostic associations between MRI-biomarkers and disease progression to provide further insights into DKD pathogenesis and risk stratification. Further studies with biopsy validation will be important to investigate whether our mpMRI protocol could non-invasively identify other/additional non-diabetic kidney disease in patients presumed to have DKD, a question of high clinical relevance.

ACKNOWLEDGEMENTS

We would like to thank Erica De Coursey and Stig Eriksson at the MRI Unit, Dept. of Radiology, SU, Gothenburg, Sweden for performing mpMRI examinations; Lotta Sundström, BMA, Inger Olander, BMA, and all physicians at Njurmedicin, SU,

Gothenburg, Sweden, and subjects who participated in this study. We are thankful to Dr Eleanor Cox from the Sir Peter Mansfield Imaging Centre, Nottingham for providing software for analysis of T1 and ASL images and to Dr Grażyna Söderbom for her technical editorial assistance.

SUPPLEMENTARY DATA

Supplementary data are available at *ckj* online.

CONFLICT OF INTEREST STATEMENT

SBA received research support for this study from Antaros Medical and AstraZeneca.

PDH, LVJ, CE and JH are employees of Antaros Medical.

AKS is an employee of AstraZeneca.

All other authors declare that there are no relationships or activities that might bias, or be perceived to bias, their contribution to this manuscript, and the results presented in this paper have not been published previously in whole or part, except in abstract format.

AUTHORS' CONTRIBUTIONS

All named authors meet the International Committee of Medical Journal Editors criteria for authorship for this article. All authors assisted in concept and design of the study, providing intellectual content of critical importance, revised and gave approval for the final version of the manuscript to be published.

SBA is the principal investigator. She participated in data acquisition, analysis and interpretation, supervision and conduct of the overall study, writing of the original draft of the article with input from others.

KM participated in data acquisition, analysis and interpretation; and writing of the original draft of the article with input from others.

PDH developed the MRI protocol together with SF, participated in data analysis and interpretation, and contributed to writing of the original draft of the article.

GE participated in data acquisition, analysis and interpretation.

TU and HL participated as radiologists in the MRI data analysis and interpretation, and identified and reported incidental findings on MRI scans.

SF developed the MRI protocol and participated in data analysis and interpretation.

FUNDING

The study was funded by Antaros Medical and AstraZeneca.

DATA AVAILABILITY STATEMENT

The data underlying this article cannot be shared publicly for the privacy of individuals that participated in the study. The data will be shared on reasonable request to the corresponding author**.**

REFERENCES

1. Fu H, Liu S, Bastacky SI, Wang X, Tian XJ, Zhou D. Diabetic kidney diseases revisited: A new perspective for a new era. Mol Metab 2019; 30:250-263.
2. Alicic RZ, Rooney MT, Tuttle KR. Diabetic Kidney Disease: Challenges, Progress, and Possibilities. Clin J Am Soc Nephrol 2017; 12:2032-2045.
3. Luis-Lima S, Porrini E. An Overview of Errors and Flaws of Estimated GFR versus True GFR in Patients with Diabetes Mellitus. Nephron 2017; 136:287-291.
4. Stevens LA, Levey AS. Measured GFR as a confirmatory test for estimated GFR. J Am Soc Nephrol 2009; 20:2305-13.
5. Jufar AH, Lankadeva YR, May CN, Cochrane AD, Bellomo R, Evans RG. Renal functional reserve: from physiological phenomenon to clinical biomarker and beyond. Am J Physiol Regul Integr Comp Physiol 2020; 319:R690-R702.
6. Waikar SS, Rebholz CM, Zheng Z, et al. Biological Variability of Estimated GFR and Albuminuria in CKD. Am J Kidney Dis 2018; 72:538-546.
7. Inker LA, Levey AS, Pandya K, et al. Early change in proteinuria as a surrogate end point for kidney disease progression: an individual patient meta-analysis. Am J Kidney Dis 2014; 64:74-85.
8. Tuttle KR, Bakris GL, Bilous RW, et al. Diabetic kidney disease: a report from an ADA Consensus Conference. Diabetes Care 2014; 37:2864-83.
9. Pugliese G, Penno G, Natali A, et al. Diabetic kidney disease: New clinical and therapeutic issues. Joint position statement of the Italian Diabetes Society and the Italian Society of Nephrology on "The natural history of diabetic kidney disease and treatment of hyperglycemia in patients with type 2 diabetes and impaired renal function". Nutr Metab Cardiovasc Dis 2019; 29:1127-1150.
10. Tervaert TW, Mooyaart AL, Amann K, et al. Pathologic classification of diabetic nephropathy. J Am Soc Nephrol 2010; 21:556-63.
11. Luciano RL, Moeckel GW. Update on the Native Kidney Biopsy: Core Curriculum 2019. Am J Kidney Dis 2019; 73:404-415.
12. Stanton RC. Clinical challenges in diagnosis and management of diabetic kidney disease. Am J Kidney Dis 2014; 63:S3-21.
13. Selby NM, Blankestijn PJ, Boor P, et al. Magnetic resonance imaging biomarkers for chronic kidney disease: a position paper from the European Cooperation in Science and Technology Action PARENCHIMA. Nephrol Dial Transplant 2018; 33:ii4-ii14.
14. Mahmoud H, Buchanan C, Francis ST, Selby NM. Imaging the kidney using magnetic resonance techniques: structure to function. Curr Opin Nephrol Hypertens 2016; 25:487-493.
15. Pruijm M, Milani B, Pivin E, et al. Reduced cortical oxygenation predicts a progressive decline of renal function in patients with chronic kidney disease. Kidney Int 2018; 93:932-940.
16. Villa G, Ringgaard S, Hermann I, et al. Phase-contrast magnetic resonance imaging to assess renal perfusion: a systematic review and statement paper. MAGMA 2020; 33:3-21.
17. Wolf M, de Boer A, Sharma K, et al. Magnetic resonance imaging T1- and T2-mapping to assess renal structure and function: a systematic review and statement paper. Nephrol Dial Transplant 2018; 33:ii41-ii50.
18. Caroli A, Pruijm M, Burnier M, Selby NM. Functional magnetic resonance imaging of the kidneys: where do we stand? The perspective of the European COST Action PARENCHIMA. Nephrol Dial Transplant 2018; 33:ii1-ii3.
19. Buchanan CE, Mahmoud H, Cox EF, et al. Quantitative assessment of renal structural and functional changes in chronic kidney disease using multi-parametric magnetic resonance imaging. Nephrol Dial Transplant 2020; 35:955-964.
20. Cakmak P, Yagci AB, Dursun B, Herek D, Fenkci SM. Renal diffusion-weighted imaging in diabetic nephropathy: correlation with clinical stages of disease. Diagn Interv Radiol 2014; 20:374-8.
21. Feng YZ, Ye YJ, Cheng ZY, et al. Non-invasive assessment of early stage diabetic nephropathy by DTI and BOLD MRI. Br J Radiol 2020; 93:20190562.

22. Mora-Gutierrez JM, Garcia-Fernandez N, Slon Roblero MF, et al. Arterial spin labeling MRI is able to detect early hemodynamic changes in diabetic nephropathy. J Magn Reson Imaging 2017; 46:1810-1817.
23. Brown RS, Sun MRM, Stillman IE, Russell TL, Rosas SE, Wei JL. The utility of magnetic resonance imaging for noninvasive evaluation of diabetic nephropathy. Nephrol Dial Transplant 2020; 35:970-978.
24. Levey AS, Stevens LA, Schmid CH, et al. A new equation to estimate glomerular filtration rate. Ann Intern Med 2009; 150:604-12.
25. Levey AS, de Jong PE, Coresh J, et al. The definition, classification, and prognosis of chronic kidney disease: a KDIGO Controversies Conference report. Kidney Int 2011; 80:17-28.
26. Krutzen E, Back SE, Nilsson-Ehle I, Nilsson-Ehle P. Plasma clearance of a new contrast agent, iohexol: a method for the assessment of glomerular filtration rate. J Lab Clin Med 1984; 104:955-61.
27. Fluss R, Faraggi D, Reiser B. Estimation of the Youden Index and its associated cutoff point. Biom J 2005; 47:458-72.
28. Shrout PE, Fleiss JL. Intraclass correlations: uses in assessing rater reliability. Psychol Bull 1979; 86:420-8.
29. Gu S, Wang A, Ning G, Zhang L, Mu Y. Insulin resistance is associated with urinary albumin-creatinine ratio in normal weight individuals with hypertension and diabetes: The REACTION study. J Diabetes 2020; 12:406-416.
30. Cox EF, Buchanan CE, Bradley CR, et al. Multiparametric Renal Magnetic Resonance Imaging: Validation, Interventions, and Alterations in Chronic Kidney Disease. Front Physiol 2017; 8:696.
31. Keegan J, Patel HC, Simpson RM, Mohiaddin RH, Firmin DN. Inter-study reproducibility of interleaved spiral phase velocity mapping of renal artery haemodynamics. J Cardiovasc Magn Reson 2015; 17:8.
32. Jiang K, Ponzo TA, Tang H, Mishra PK, Macura SI, Lerman LO. Multiparametric MRI detects longitudinal evolution of folic acid-induced nephropathy in mice. Am J Physiol Renal Physiol 2018; 315:F1252-F1260.
33. Li A, Xu C, Liang P, et al. Role of Chemical Exchange Saturation Transfer and Magnetization Transfer MRI in Detecting Metabolic and Structural Changes of Renal Fibrosis in an Animal Model at 3T. Korean J Radiol 2020; 21:588-597.
34. de Boer A, Harteveld AA, Stemkens B, et al. Multiparametric Renal MRI: An Intrasubject Test-Retest Repeatability Study. J Magn Reson Imaging 2021; 53:859-873.
35. Wittsack HJ, Lanzman RS, Quentin M, et al. Temporally resolved electrocardiogram-triggered diffusion-weighted imaging of the human kidney: correlation between intravoxel incoherent motion parameters and renal blood flow at different time points of the cardiac cycle. Invest Radiol 2012; 47:226-30.
36. Field M PC, Harris D. Glomerular Filtration in acute kidney injury. The Renal System. 2010, 57-68.
37. Fananapazir G, Benzl R, Corwin MT, et al. Predonation Volume of Future Remnant Cortical Kidney Helps Predict Postdonation Renal Function in Live Kidney Donors. Radiology 2018; 288:153-157.
38. Halleck F, Diederichs G, Koehlitz T, et al. Volume matters: CT-based renal cortex volume measurement in the evaluation of living kidney donors. Transpl Int 2013; 26:1208-16.
39. Emamian SA, Nielsen MB, Pedersen JF, Ytte L. Kidney dimensions at sonography: correlation with age, sex, and habitus in 665 adult volunteers. AJR Am J Roentgenol 1993; 160:83-6.
40. Levey AS, Gansevoort RT, Coresh J, et al. Change in Albuminuria and GFR as End Points for Clinical Trials in Early Stages of CKD: A Scientific Workshop Sponsored by the National Kidney Foundation in Collaboration With the US Food and Drug Administration and European Medicines Agency. Am J Kidney Dis 2020; 75:84-104.
41. Clodagh M SM, Dhanda R. Renal physiology: blood flow, glomerular filtration and plasma clearance. Anaesthesia & Intensive Care Medicine 2018:254-257.

42. Hanamura K, Tojo A, Kinugasa S, Asaba K, Fujita T. The resistive index is a marker of renal function, pathology, prognosis, and responsiveness to steroid therapy in chronic kidney disease patients. Int J Nephrol 2012; 2012:139565.
43. Kim JH, Lee SM, Son YK, Kim SE, An WS. Resistive index as a predictor of renal progression in patients with moderate renal dysfunction regardless of angiotensin converting enzyme inhibitor or angiotensin receptor antagonist medication. Kidney Res Clin Pract 2017; 36:58-67.
44. Sistani SS, Alidadi A, Moghadam AA, Mohamadnezhad F, Ghahderijani BH. Comparison of renal arterial resistive index in type 2 diabetic nephropathy stage 0-4. Eur J Transl Myol 2019; 29:8364.
45. Solini A, Giannini L, Seghieri M, et al. Dapagliflozin acutely improves endothelial dysfunction, reduces aortic stiffness and renal resistive index in type 2 diabetic patients: a pilot study. Cardiovasc Diabetol 2017; 16:138.
46. Pruijm M, Milani B, Burnier M. Blood Oxygenation Level-Dependent MRI to Assess Renal Oxygenation in Renal Diseases: Progresses and Challenges. Front Physiol 2016; 7:667.
47. Bane O, Mendichovszky IA, Milani B, et al. Consensus-based technical recommendations for clinical translation of renal BOLD MRI. MAGMA 2020; 33:199-215.
48. Sugiyama K, Inoue T, Kozawa E, et al. Reduced oxygenation but not fibrosis defined by functional magnetic resonance imaging predicts the long-term progression of chronic kidney disease. Nephrol Dial Transplant 2020; 35:964-970.
49. Zhou H, Yang M, Jiang Z, Ding J, Di J, Cui L. Renal Hypoxia: An Important Prognostic Marker in Patients with Chronic Kidney Disease. Am J Nephrol 2018; 48:46-55.
50. Prasad PV, Li LP, Thacker JM, et al. Cortical Perfusion and Tubular Function as Evaluated by Magnetic Resonance Imaging Correlates with Annual Loss in Renal Function in Moderate Chronic Kidney Disease. Am J Nephrol 2019; 49:114-124.

Table 1. Inclusion/exclusion criteria

Inclusion criteria	Exclusion criteria
DKD subjects	
Signed informed consent	Cause for the impaired kidney function diagnosed primarily to be other than DKD (histologic or clinical)
Age 18-79 years	History of renal transplant
T2DM with clinical diagnosis of DKD and an eGFR between 15-60 ml/min/1.73 m^2	Patients with congestive heart failure (NYHA class IV)
UACR >3 mg/mmol in the first morning urine sample	Pregnancy
An eGFR decline of <10 ml/min/1.73 m^2 over last 6 months	Any contraindication for MRI examination e.g., pacemaker, severe claustrophobia
Stable dose of anti-diabetic treatment for >1 month	Allergy to iodine-based contrast agents
BMI 18-35	Involved in the planning or execution of this study
Healthy volunteers	
Signed informed consent	HIV/hepatitis B- or C- positive
Age 18-79 years	Evidence of any active or chronic disease following a detailed medical history including but not limited to T2DM, congestive heart failure (NYHA 3 and 4) and hypertension
eGFR >70 ml/min/1.73 m^2	Pregnancy
UACR <3 mg/mmol	Any contraindication for MRI examination e.g., pacemaker, severe claustrophobia
BMI 18-35	Allergy to iodine-based contrast agents
Not receiving any medical treatment	Involved in the planning or execution of this study
BMI=Body Mass Index; DKD= Diabetic Kidney Disease; eGFR= estimated Glomerular Filtration Rate; HIV= Human Immunodeficiency Virus; NYHA= New York Heart Association classification; mGFR= measured Glomerular Filtration Rate; T2DM= Type 2 Diabetes Mellitus; UACR= Urine Albumin-to-Creatinine Ratio.	

Table 2. Imaging variables measured in the mpMRI protocol

Variable	Assessment
Kidney Hemodynamics[13,38,39]	
Phase Contrast (PC) MRI	
Peak systolic and diastolic velocity [cm/s]	Peak blood velocity in the renal artery in systole and diastole.
Renal Artery Resistive Index (RARI) [no unit]	Measures the resistance of renal arterial flow to the kidney.
Mean arterial flow (MAF) [mL/min]	Mean blood flow in the renal artery.
Global Perfusion [ml/min/100g]	Mean renal flow per 100g of kidney tissue.
Arterial Spin Labelling (ASL) [ml/100g/min][38]	Uses the magnetic labelling of water in arterial blood as an endogenous tracer to generate maps of regional kidney perfusion.
Kidney Macrostructure[40]	
Kidney volume [mL]	Volume of kidney parenchyma from T_2-weighted structural images.
Kidney Oxygenation with Blood Oxygen Level Dependent (BOLD) MRI[22,41]	
BOLD R_2* [s^{-1}]	Allows indirect assessment of tissue oxygenation based on the paramagnetic properties of endogenous deoxyhemoglobin.
Kidney Microstructure[19,26,42]	
Apparent Diffusion Coefficient (ADC) [mm^2s^{-1} x 10^{-3}]	Relates to interstitial fibrosis by measuring the restriction of water displacement seen on diffusion weighted imaging (DWI).
Intravoxel Incoherent motion (IVIM) parameters [s^{-1}][19] Fast component of diffusion (pseudo-perfusion) D* [mm^2s^-1 x 10^{-3}] Slow component of diffusion D [mm^2s^-1 x 10^{-3}] Perfusion fraction f [%]	IVIM separates the intracellular water diffusion (D) and vascular perfusion (D*) components of the ADC measurement.
R_1 [s^{-1}][26]	Longitudinal Nuclear Magnetic Resonance relaxation rate (R_1) of water reflects the molecular environment, for example, viscosity, fibrosis and inflammation (interstitial oedema, cellular swelling). $R_1=1/T_1$
Magnetization Transfer Contrast (MTC) [%][43]	Measurement of the energy interaction of large macromolecules and bulk water protons which has been shown to correlate with fibrosis.

Table 3. Baseline characteristics of the DKD and HV groups

Variable	HV (n=20)	Stage G3 (n=16)	Stage G4/5 (n=20)	Stage G3–G5 (n=36)
Age (years)	66.7 (6.2)	68.9 (5.6)	68.3 (5.6)	68.6 (5.5)
Ethnicity (no. Caucasian [%])	20 (100%)	16 (100%)	18 (90%)	34 (94%)
Gender (no. male [%])	15 (75%)	12 (75%)	18 (90%)	30 (83%)
BMI (kg/m^2)	25.5 (3.1)	28 (3.3)	27.8 (3.0)	27.9 (3.1)
Systolic blood pressure (mmHg)	133 (12)	147 (21)	153 (22)	150 (21)
Diastolic blood pressure (mmHg)	80.4 (7.3)	80.1 (9.4)	78 (7.9)	78.9 (8.5)
Hemoglobin (g/L)	145 (12.0)	134 (11.6)	133.2 (16.1)	134 (14.1)
Creatinine (µmol/L)	82 (12)	135 (29)	230 (54)	188 (65)
UACR ratio (mg/mmol)	1.2 (0.7)	34.1 (44.3)	85 (81.0)	62.4 (71.1)
eGFR ($mL/min/1.73m^2$)	79.1 (7.2)	45.3 (10.7)	25 (5.6)	34 (13.1)
mGFR ($mL/min/1.73m^2$)	81.5 (9.2)	40.4 (6.7)	21.8 (4.7)	30.1 (10.9)
HbA1c (mmol/mol)	35.6 (3.3)	54.2 (11.6)	62.2 (14.1)	58.6 (13.5)
Use of RAAS blockers, n (%)	0.0 (0%)	12 (75%)	14 (70%)	26 (72%)
Hypertension, n (%)	0.0 (0%)	14 (88%)	20 (100%)	34 (94%)

Data are presented as n (%) or mean (SD). BMI=Body Mass Index; eGFR= estimated Glomerular Filtration Rate; mGFR= measured Glomerular Filtration Rate; RAAS= Renin Angiotensin Aldosterone System; UACR= Urine Albumin-to-Creatinine Ratio. GFR stages were stratified by mGFR.

Table 4. Descriptive statistics and predictive properties (ROC AUC) of univariate imaging markers to distinguish between DKD subjects (stages G3–G5) and HV, including respective specificity and sensitivity for Youden cut-off values

	HV		DKD (Stages G3–G5)		Prediction Performance				
Variable	**N**	**Mean (SD)**	**N**	**Mean (SD)**	**ROC AUC**	**Cut-off**	**Sensitivity**	**Specificity**	***P-value**
Kidney Hemodynamics									
MAF (ml/min/1.73m^2)	20	993 (126)	36	538 (161)	0.99	<803	0.94	1.00	0.04
Peak systolic velocity (cm/s)	20	54.3 (8.28)	36	50.5 (15.0)	0.62	<48.3	0.53	0.85	0.30
End diastolic velocity (cm/s)	20	17.0 (3.9)	36	8.75 (3.6)	0.94	<12.6	0.89	0.90	0.0005
RARI	20	0.68 (0.06)	36	0.82 (0.06)	0.94	>0.73	0.94	0.85	0.0001
ASL perfusion cortex (ml/min/100g)	20	164 (36.8)	35	81.1 (40.7)	0.93	<125	0.86	0.90	0.0001
Global Perfusion (ml/min/100g)	20	458 (54)	36	311 (83)	0.94	<380	0.81	0.95	0.001
Kidney Macrostructure									
Kidney volume (ml/1.73m^2)	20	218 (26)	36	176 (38)	0.83	<206	0.83	0.75	0.0008
Kidney Oxygenation									
BOLD R_2* cortex (s^{-1})	20	17.3 (1.4)	33	17.1 (1.4)	0.52	<16.6	0.36	0.80	0.53
BOLD R_2* medulla (s^{-1})	20	26.0 (2.3)	33	23.5 (3.7)	0.75	<22.6	0.48	1.00	0.002
Kidney Microstructure									
ADC cortex (10-3 mm^2s^{-1})	20	2.52 (0.19)	34	2.31 (0.21)	0.79	<2.37	0.71	0.85	0.002
ADC medulla (10-3 mm^2s^{-1})	20	2.33 (0.18)	34	2.19 (0.24)	0.71	<2.21	0.65	0.75	0.03
R_1 cortex (s^{-1})	20	0.72 (0.03)	36	0.63 (0.04)	0.97	<0.69	0.94	0.90	0.001
R_1 medulla (s^{-1})	20	0.55 (0.02)	36	0.55 (0.02)	0.58	<0.55	0.56	0.65	0.34
IVIM Slow Diffusion (D) cortex (10^{-3} mm^2s^{-1})	20	2.14 (0.24)	34	1.91 (0.26)	0.75	<1.98	0.65	0.80	0.006
IVIM Slow Diffusion (D) medulla (10^{-3} mm^2s^{-1})	20	2.04 (0.27)	34	1.85 (0.20)	0.72	<2.05	0.91	0.45	0.01
IVIM Fast Diffusion (D*) cortex (10^{-3} mm^2s^{-1})	19	56 (73.3)	32	98 (351)	0.48	>19.4	0.72	0.37	0.62
IVIM Fast Diffusion (D*) medulla (10^{-3} mm^2s^{-1})	19	198 (459)	31	190 (768)	0.55	<165	0.90	0.26	0.96

IVIM Perfusion Fraction (f) cortex (%)	19	13.5 (5.7)	32	15.2 (5.7)	0.60	>15	0.53	0.74	0.32
IVIM Perfusion Fraction (f) medulla (%)	19	12.3 (5.1)	31	14.5 (5.7)	0.62	>13.5	0.61	0.74	0.17
MTR cortex (%)	20	23 (1.9)	36	21.8 (2.2)	0.66	<21.7	0.56	0.80	0.06
MTR medulla (%)	20	24.5 (2.13)	36	23.7 (2.43)	0.57	<22.5	0.42	0.85	0.27
Biochemistry									
eGFR (mL/min/1.73m^2)	20	76.4 (7.76)	36	34.9 (13.8)	0.99	<60	0.97	1.00	0.02
UACR ratio (mg/mmol)	20	1.17 (0.54)	36	67 (83.3)	1.00	>1.9	1.00	1.00	0.02

Data are presented as n (%) or mean (SD). ADC = Apparent Diffusion Coefficient; ASL = Arterial Spin Labelling; AUC ROC = Area Under the Receiver Operating Characteristic (ROC) Curve; DKD = Diabetic Kidney Disease; eGFR = estimated Glomerular Filtration Rate; HV = Healthy Volunteers (controls); IVIM = Intravoxel Incoherent motion; MAF = Mean arterial flow; MTR = Magnetization Transfer Ratio; MRI = Magnetic Resonance Imaging; OR = Odds Ratio; RARI = Renal Artery Resistive Index; UACR = Urine Albumin-to-Creatinine Ratio.*P-value of OR=1 for the variable (Wald test) in the model. Note that P-values are inappropriate in cases when there is complete (or quasi-complete) separation of data points, i.e., when sensitivity and specificity=1 (or close to 1).

Table 5. Descriptive statistics and predictive properties (ROC AUC) of univariate imaging markers to distinguish between stage G3 and stages G4/5 in subjects with DKD, including respective specificity and sensitivity for Youden cut-off values

	Stage G3		Stages G4/5		Prediction Performance				
Variable	N	Mean (SD)	N	Mean (SD)	ROC AUC	Cut-off	Sensitivity	Specificity	*P-value
Kidney Hemodynamics									
MAF (ml/min/1.73m^2)	16	653 (133)	20	447 (118)	0.88	<605	1.00	0.69	0.004
Peak systolic velocity (cm/s)	16	59.8 (14.2)	20	43.1 (11.1)	0.83	<53.2	0.90	0.69	0.005
End diastolic velocity (cm/s)	16	11.3 (3.2)	20	6.72 (2.5)	0.87	<8.35	0.90	0.81	0.002
RARI	16	0.81 (0.06)	20	0.84 (0.06)	0.68	>0.84	0.60	0.81	0.11
ASL perfusion cortex (ml/min/100g)	16	96.4 (39.7)	19	68.2 (37.8)	0.72	<79	0.79	0.69	0.05
Global Perfusion (ml/min/100g)	16	352 (43)	20	278 (93)	0.76	<305	0.75	0.81	0.01
Kidney Macrostructure									
Kidney volume (ml/1.73m^2)	16	185 (27.8)	20	169 (43.4)	0.63	<155	0.40	0.94	0.20
Kidney Oxygenation									
BOLD R_2* cortex (s^{-1})	15	17.2 (1.6)	18	17 (1.25)	0.51	<16.1	0.28	0.87	0.56
BOLD R_2* medulla (s^{-1})	15	24.5 (3.7)	18	22.8 (3.6)	0.64	<23.5	0.72	0.60	0.19
Kidney Microstructure									
ADC cortex (10-3 mm^2s^{-1})	15	2.37 (0.17)	19	2.27 (0.22)	0.67	<2.32	0.68	0.73	0.18
ADC medulla (10-3 mm^2s^{-1})	15	2.21 (0.24)	19	2.17 (0.24)	0.59	<2.21	0.74	0.60	0.58
R_1 cortex (s^{-1})	16	0.65 (0.03)	20	0.62 (0.04)	0.76	<0.62	0.50	0.94	0.02
R_1 medulla (s^{-1})	16	0.55 (0.02)	20	0.54 (0.02)	0.70	<0.55	0.80	0.63	0.06
IVIM Slow Diffusion (D) cortex (10^{-3} mm^2s^{-1})	15	1.96 (0.17)	19	1.87 (0.32)	0.62	<1.91	0.63	0.73	0.30
IVIM Slow Diffusion (D) medulla (10^{-3} mm^2s^{-1})	15	1.86 (0.17)	19	1.85 (0.23)	0.51	<1.72	0.37	0.80	0.87
IVIM Fast Diffusion (D*) cortex (10^{-3} mm^2s^{-1})	15	48.2 (48.5)	17	143 (482)	0.42	>2010	0.06	1.00	0.52
IVIM Fast Diffusion (D*) medulla (10^{-3} mm^2s^{-1})	14	48.7 (58.6)	17	306 (1035)	0.53	>19.5	0.76	0.50	0.69
IVIM Perfusion Fraction	15	14.7 (5.13)	17	15.6 (6.3)	0.51	>12.3	0.82	0.33	0.66

(f) cortex (%)									
IVIM Perfusion Fraction (f) medulla (%)	14	14.6 (5.59)	17	14.3 (5.9)	0.52	<12	0.47	0.71	0.89
MTR cortex (%)	16	21.6 (2.41)	20	22 (2.0)	0.54	>20.7	0.75	0.38	0.57
MTR medulla (%)	16	23.6 (2.35)	20	23.9 (2.6)	0.52	>22.2	0.70	0.44	0.75
Biochemistry									
eGFR (mL/min/1.73m^2)	16	46.3 (12.1)	20	25.9 (6.3)	0.96	<31	0.85	0.94	0.008
UACR ratio (mg/mmol)	16	33 (47)	20	94.2 (97)	0.72	>97	0.45	0.94	0.05

Data are presented as n (%) or mean (SD). ADC = Apparent Diffusion Coefficient; ASL = Arterial Spin Labelling; AUC ROC = Area Under the Receiver Operating Characteristic (ROC) Curve; DKD = Diabetic Kidney Disease; eGFR = estimated Glomerular Filtration Rate; HV = Healthy Volunteers (controls); IVIM = Intravoxel Incoherent motion; MAF = Mean arterial flow; MTR = Magnetization Transfer Ratio; MRI = Magnetic Resonance Imaging; OR = Odds Ratio; RARI = Renal Artery Resistive Index; UACR = Urine Albumin-to-Creatinine Ratio. GFR stages were stratified by mGFR.

*P-value of OR = 1 for the variable (Wald test) in the model. Note that P-values are inappropriate in cases when there is complete (or quasi-complete) separation of data points, i.e., when sensitivity and specificity = 1 (or close to 1).

Table 6. Intra-Individual Coefficient of Variance and Intra-Class Correlation Coefficient values for the evaluation of data repeatability of MRI-biomarkers in HV and DKD subjects

Variable	CV	ICC
Kidney Hemodynamics		
MAF (ml/min/1.73m^2)	0.07	0.97
Peak systolic velocity (cm/s)	0.09	0.90
End diastolic velocity (cm/s)	0.12	0.96
RARI	0.02	0.96
ASL perfusion cortex (ml/min/100g)	0.33	0.71
Global Perfusion (ml/min/100g)	0.09	0.92
Kidney Macrostructure		
Kidney volume (ml/1.73m^2)	0.07	0.89
Kidney Oxygenation		
BOLD R_2* cortex (s^{-1})	0.04	0.74
BOLD R_2* medulla (s^{-1})	0.05	0.90
Kidney Microstructure		
ADC cortex (10^{-3} mm^2s^{-1})	0.06	0.66
ADC medulla (10^{-3} mm^2s^{-1})	0.05	0.66
R_1 cortex (s^{-1})	0.02	0.94
R_1 medulla (s^{-1})	0.02	0.49
IVIM Slow Diffusion (D) cortex (10^{-3} mm^2s^{-1})	0.11	0.29
IVIM Slow Diffusion (D) medulla (10^{-3} mm^2s^{-1})	0.09	0.37
IVIM Fast Diffusion (D*) cortex (10^{-3} mm^2s^{-1})	4.97	0.00
IVIM Fast Diffusion (D*) medulla (10^{-3} mm^2s^{-1})	5.30	0.00
IVIM Perfusion Fraction (f) cortex (%)	0.30	0.21
IVIM Perfusion Fraction (f) medulla (%)	0.25	0.46
MTR cortex (%)	0.08	0.31
MTR medulla (%)	0.11	0.01
Biochemistry		
eGFR (mL/min/1.73m^2)	0.06	0.99
UACR ratio (mg/mmol)	0.28	0.96

Data are presented as n (%) or mean (SD). ADC = Apparent Diffusion Coefficient; ASL = Arterial Spin Labelling; CV = Intra-Individual Coefficient of Variance; DKD = Diabetic Kidney Disease; HV = Healthy Volunteers (controls); ICC = Intra-Class Correlation Coefficient, type (2,1); IVIM = Intravoxel Incoherent Motion; eGFR = estimated Glomerular Filtration Rate, MAF = Mean arterial flow; MRI = Magnetic Resonance Imaging; MTR = Magnetization Transfer Ratio; OR = Odds Ratio; RARI = Renal Artery Resistive Index; UACR = Urine Albumin-to-Creatinine Ratio.

Table 7. The correlation between mGFR and UACR, and MRI-biomarkers of kidney hemodynamics, macro- and micro-structure, and oxygenation

	mGFR		UACR		UACR (Bivariate analysis with mGFR + imaging variable)	
Variable	**Pearson correlation (r)**	***P-value**	**Spearman correlation (r)**	****P-value**	**Pearson correlation (r^2)**	*****P-value**
mGFR			-0.81	<0.0001	0.15	0.02
Kidney Hemodynamics						
MAF (ml/min/1.73m^2)	0.92	<0.0001	-0.78	<0.0001	0.16	0.63
Peak systolic velocity (cm/s)	0.32	0.02	-0.28	0.03	0.15	0.95
End diastolic velocity (cm/s)	0.79	<0.0001	-0.75	<0.0001	0.23	0.07
RARI	-0.76	<0.0001	0.70	<0.0001	0.21	0.13
ASL perfusion cortex (ml/min/100g)	0.70	<0.0001	-0.65	<0.0001	0.15	0.51
Global Perfusion (ml/min/100g)	0.75	<0.0001	-0.63	<0.0001	0.16	0.59
Kidney Macrostructure						
Kidney volume (ml/1.73m^2)	0.61	<0.0001	-0.50	<0.0001	0.16	0.49
Kidney Oxygenation						
BOLD R_2* cortex (s^{-1})	0.07	0.59	-0.11	0.41	0.14	0.82
BOLD R_2* medulla (s^{-1})	0.35	0.008	-0.34	0.01	0.23	0.06
Kidney Microstucture						
ADC cortex (10-3 mm^2s^{-1})	0.48	0.0002	-0.37	0.005	0.21	0.36
ADC medulla (10-3 mm^2s^{-1})	0.28	0.03	-0.27	0.05	0.23	0.20
R_1 cortex (s^{-1})	0.78	<0.0001	-0.82	<0.0001	0.36	0.003
R_1 medulla (s^{-1})	0.20	0.13	-0.33	0.01	0.25	0.04
IVIM Slow Diffusion (D) cortex (10^{-3} mm^2s^{-1})	0.44	0.0007	-0.27	0.04	0.30	0.03
IVIM Slow Diffusion (D) medulla (10^{-3} mm^2s^{-1})	0.35	0.007	-0.23	0.08	0.24	0.15
IVIM Fast Diffusion (D*) cortex (10^{-3} mm^2s^{-1})	-0.09	0.54	-0.12	0.38	0.19	0.47
IVIM Fast Diffusion (D*) medulla (10^{-3} mm^2s^{-1})	-0.00	1.00	-0.18	0.19	0.15	0.44

IVIM Perfusion Fraction (f) cortex (%)	-0.17	0.23	0.09	0.54	0.37	0.005
IVIM Perfusion Fraction (f) medulla (%)	-0.21	0.13	0.17	0.22	0.19	0.17
MTR cortex (%)	0.23	0.09	-0.26	0.05	0.15	0.74
MTR medulla (%)	0.13	0.34	-0.14	0.30	0.15	0.82

Univariate linear regression was used to evaluate the linear association of each MRI-biomarker with mGFR and UACR (mGFR or UACR as a dependent variable, MRI-biomarker as an independent variable). Bivariate predictors of UACR were examined using mGFR as one variable and adding one MRI endpoint using linear regression only in the DKD subjects. Data are presented as n /%) or mean (SD). ADC = Apparent Diffusion Coefficient; ASL = Arterial Spin Labelling; IVIM = Intravoxel Incoherent Motion; mGFR = measured Glomerular Filtration Rate; MAF = Mean arterial flow; MRI = Magnetic Resonance Imaging; MTR = Magnetization Transfer Ratio; RARI = Renal Artery Resistive Index; UACR = Urine Albumin-to-Creatinine Ratio.

Table 8. Comparison of MRI-biomarkers between study values and literature values

Study reference:		Current Study			Buchanan et al. (19)		de Boer et al. (34)	
Study subject summary:		20 HV, median age 67.0 (52.0-78.0) yr	36 DKD, stages G3–5	20 HV + 36 DKD	22 CKD subjects, stages G3, G4		19 HV, median age 49.0 (45.0–57.0) yr	
Variable	**Unit**	**Mean ± SD**	**Mean ± SD**	**CV (%)**	**Mean ± SD or median (IQR)**	**CV (%)**	**Mean ± SD**	**CV (%)**
Kidney Hemodynamics								
MAF	ml/min/1.73 m^2	993 ± 126*	538 ± 161*	7	490 (170)**	18	388 ± 147***	13
ASL perfusion cortex	ml/min/100g	164 ± 36.8	81.1 ± 40.8	33	71 (50)	23	340 ± 51	10
Global Perfusion	ml/min/100g	458 ± 53.8	311 ± 82.9	9	130 (110)	18	Not measured	Not measured
Kidney Macrostructure								
Kidney volume	ml/1.73m^2	218 ± 25.7	176 ± 37.7	7	170 (39)**	3.8	Not measured	Not measured
Kidney Oxygenation								
BOLD R_2* cortex	s^{-1}	17.3 ± 1.35	17.1 ± 1.41	4	20.0 ± 3.2	4.6	19.3 ± 2.1	6.1
BOLD R_2* medulla	s^{-1}	26.0 ± 2.31	23.5 ± 3.70	5	33.0 ± 8.0	6.8	26.2 ± 2.7	5.8
Kidney Microstructure								
ADC cortex	10^{-3} mm^2s^{-1}	2.52 ± 0.19	2.31 ± 0.21	6	2.0 (0.2)	5.3	Not measured	Not measured
ADC medulla	10^{-3} mm^2s^{-1}	2.33 ± 0.18	2.19 ± 0.24	5	2.0 ± 0.2	14	Not measured	Not measured
R_1 cortex	s^{-1}	0.72 ± 0.03	0.63 ± 0.04	2	0.64 ± 0.06	2.9	0.66 ± 0.05	5.1
R_1 medulla	s^{-1}	0.55 ± 0.02	0.55 ± 0.02	2	0.57 ± 0.03	3.9	0.53 ± 0.03	2.8
IVIM Slow Diffusion (D) cortex	10^{-3} mm^2s^{-1}	2.14 ± 0.24	1.91 ± 0.26	11	1.7 ± 0.2	7.7	2.1 ± 0.1	6.7
IVIM Slow Diffusion (D) medulla	10^{-3} mm^2s^{-1}	2.04 ± 0.27	1.85 ± 0.20	9	1.8 ± 0.2	22	1.9 ± 0.1	7.2
IVIM Perfusion Fraction (f) cortex	%	13.5 ± 5.71	15.2 ± 5.70	30	Not measured	Not measured	10 ± 3	24
IVIM Perfusion Fraction (f) medulla	%	12.3 ± 5.11	14.5 ± 5.66	25	Not measured	Not measured	13 ± 3	18
* total for both kidneys ** not corrected for BSA *** per kidney								

Data are presented as n (%) or mean (SD). ADC = Apparent Diffusion Coefficient; ASL = Arterial Spin Labelling; BSA = Body Surface Area; CV = Intra-Individual Coefficient of Variance; DKD = Diabetic Kidney Disease; HV = Healthy Volunteers (controls); IQR = Interquartile range; IVIM = Intravoxel Incoherent Motion; MAF = Mean arterial flow.

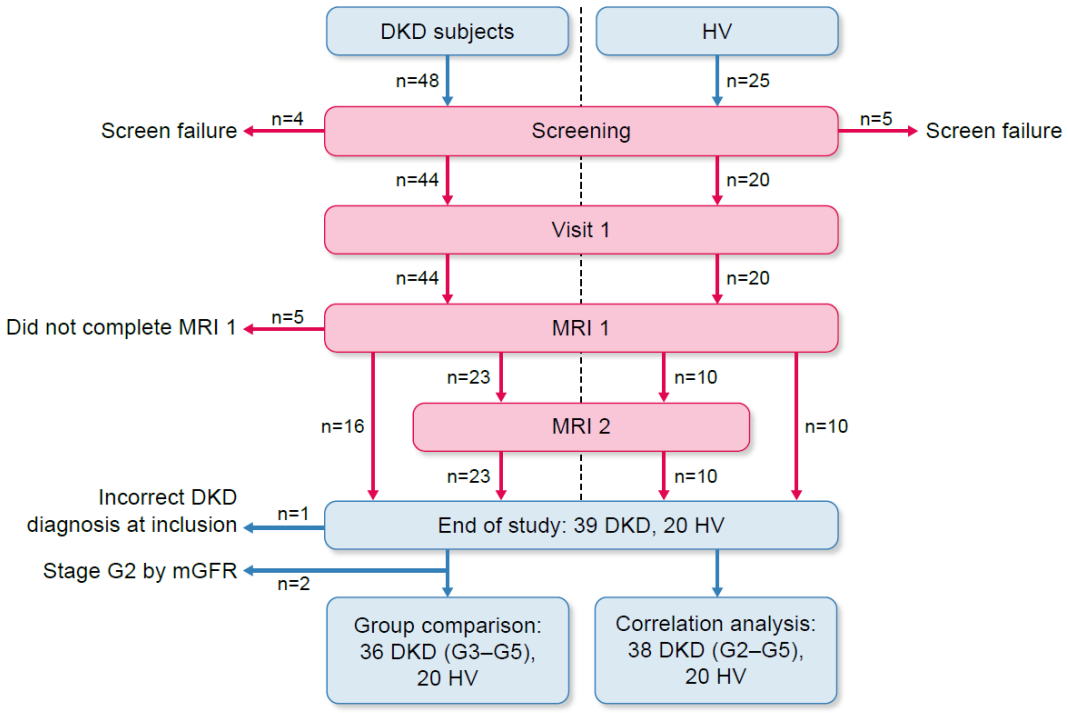

Figure 1. Study Flow Chart. A total of 48 DKD subjects were screened, n=4 did not fulfil the eligibility criteria and n=5 did not complete the study, leaving a total of 39 DKD subjects at the end of the study. Of these, 36 subjects were included in the group comparison and 38 subjects in the correlation analysis. During the same enrolment period, 25 HV were screened, 20 HV were included and completed the study.

Where: DKD = Diabetic Kidney Disease; HV = Healthy Volunteers (controls); mGFR = measured Glomerular Filtration Rate; MRI = Magnetic Resonance Imaging.

Figure 2

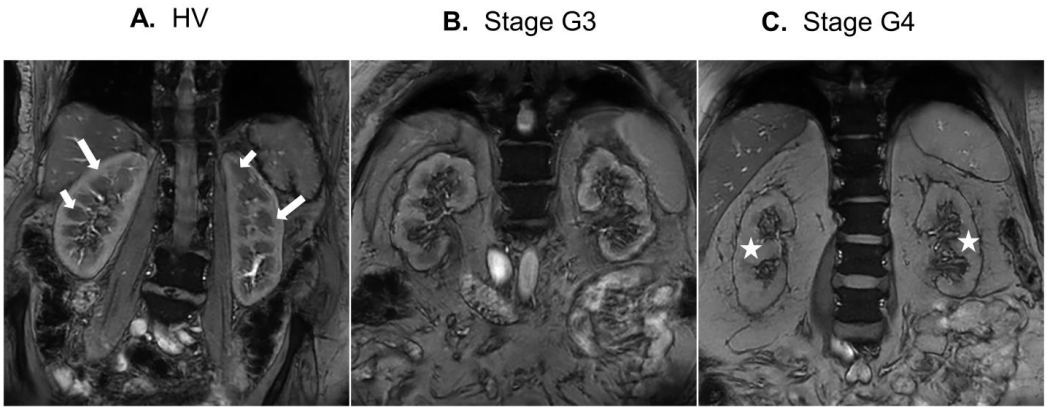

Figure 2. Anatomical T_1-weighted image of A) a typical HV (left), B) a DKD subject with GFR stage G3 (center), and C) a DKD subject with GFR stage G4 (right). Where: DKD = Diabetic Kidney Disease; GFR = Glomerular Filtration Rate; HV = Healthy Volunteers. Long white arrow = renal cortex; short white arrow = renal medulla; star = region with loss of corticomedullary contrast.

Figure 3

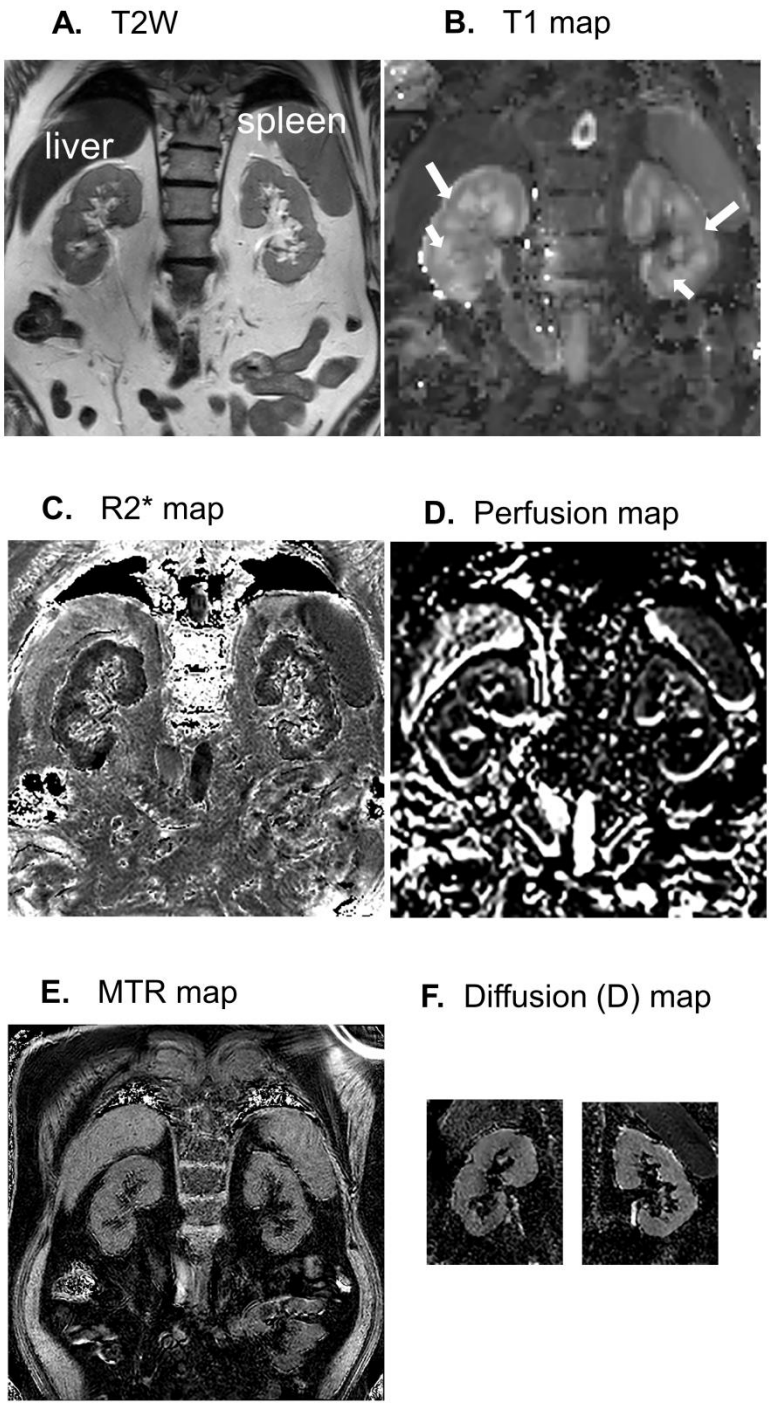

Figure 3. Representative images from a G3 subject showing A) T2 weighted (T2W) image, B) T1 map, C) R2* map, D) perfusion map (ASL), E) MTR map, and F) D

(Tissue Diffusion Coefficient) map. Note that the D maps were created following realignment of a cropped version of the DWI data set and therefore a D map of the whole slice is not available. Where: MTR= Magnetization Transfer Ratio; DWI= Diffusion Weighted Imaging. Long white arrow = renal cortex; short white arrow = renal medulla.

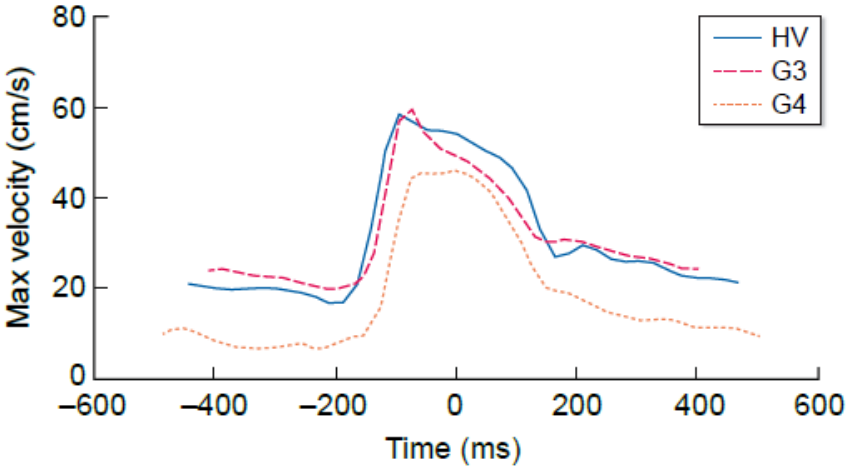

Figure 4. Representative phase contrast flow profiles through the cardiac cycle showing maximum velocity in the renal artery from a HV (—), stage G3 (**- - -**), and a stage G4 (·····) subject. Where: HV = Healthy Volunteers.

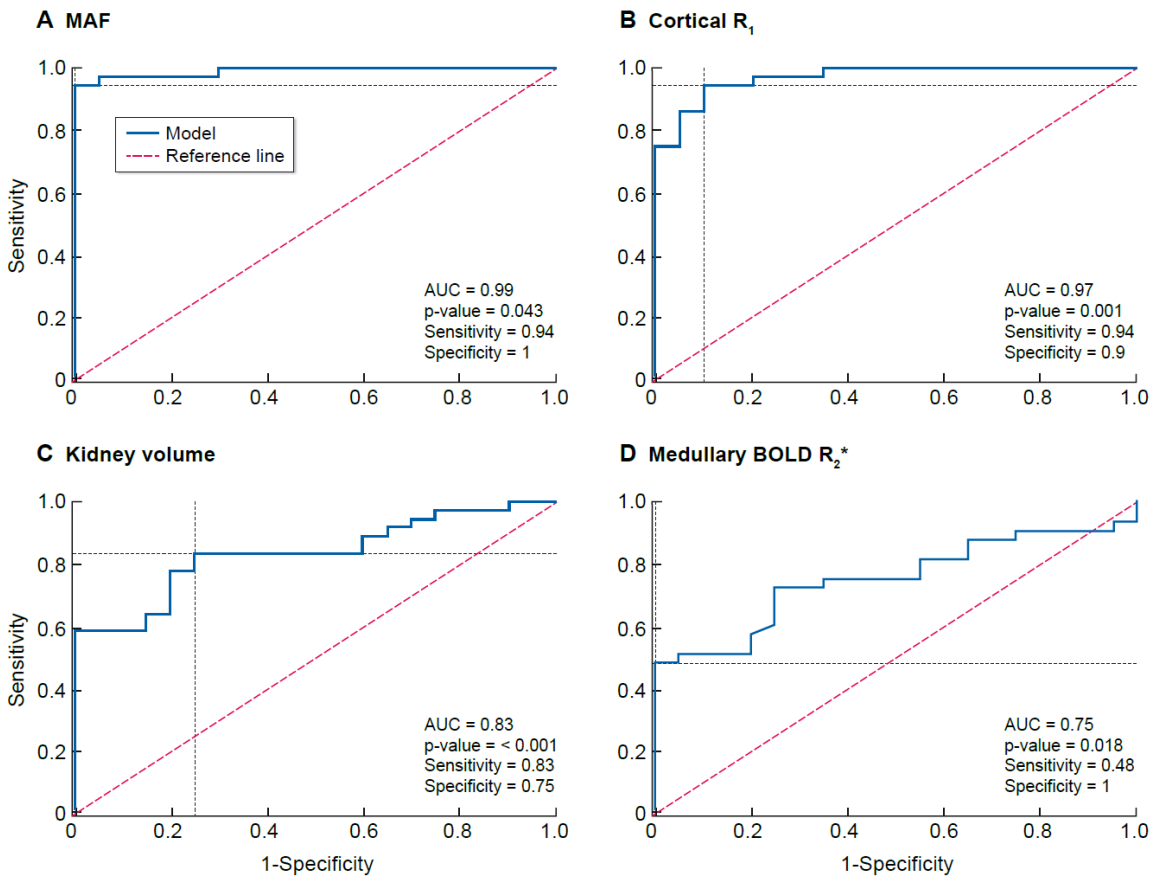

Figure 5. Receiver Operating Characteristic curves predicting separation of HV versus DKD subjects using MRI measures: A) MAF, B) Cortical R_1, C) Kidney Volume, and D) Medullary BOLD R_2*. Where: AUC ROC = Area Under the Receiver Operating Characteristic (ROC) Curve; DKD = Diabetic Kidney Disease; HV = Healthy Volunteers (controls); MAF = Mean Arterial Flow.

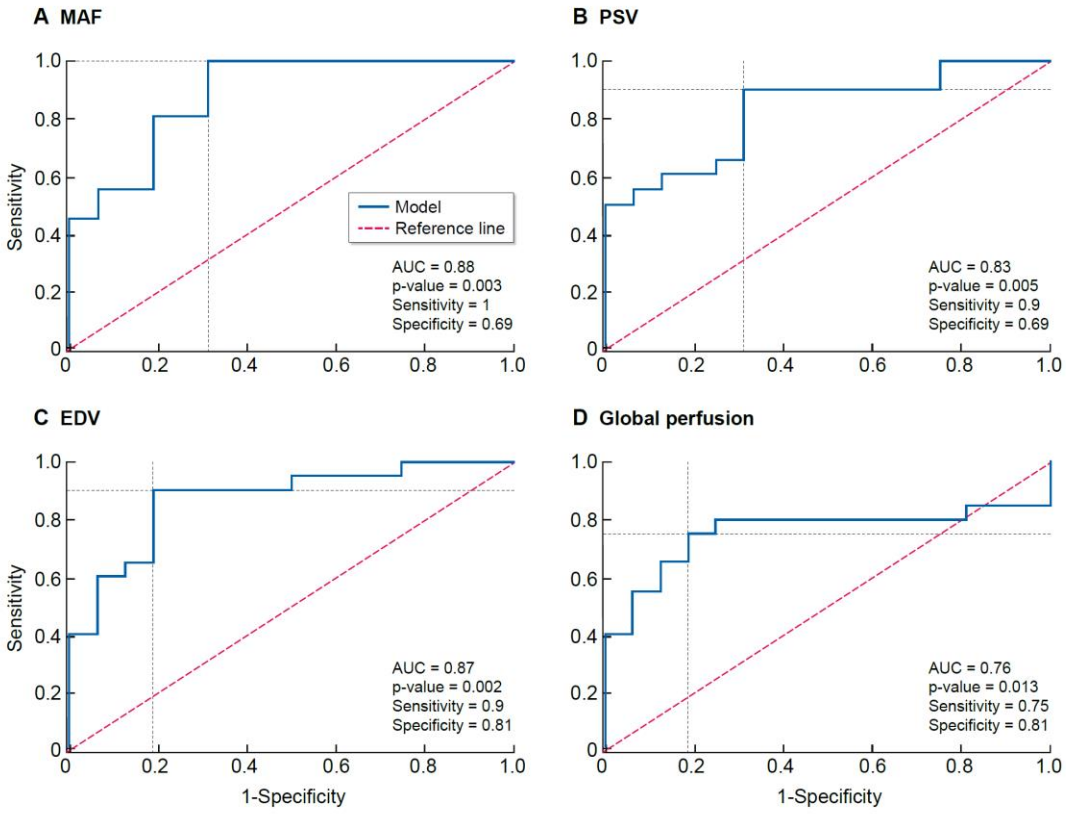

Figure 6. Receiver Operating Characteristic curves predicting separation of DKD subjects with GFR stage G3 versus stages G4/5 using MRI-biomarkers of kidney hemodynamics: A) MAF, B) Peak Systolic Velocity (PSV), C) End Diastolic Velocity (EDV), D) Global Perfusion. Where: AUC ROC = Area Under the Receiver Operating Characteristic (ROC) Curve; DKD = Diabetic Kidney Disease; GFR = Glomerular Filtration Rate; MAF = Mean Arterial Flow. GFR stages were stratified by mGFR.

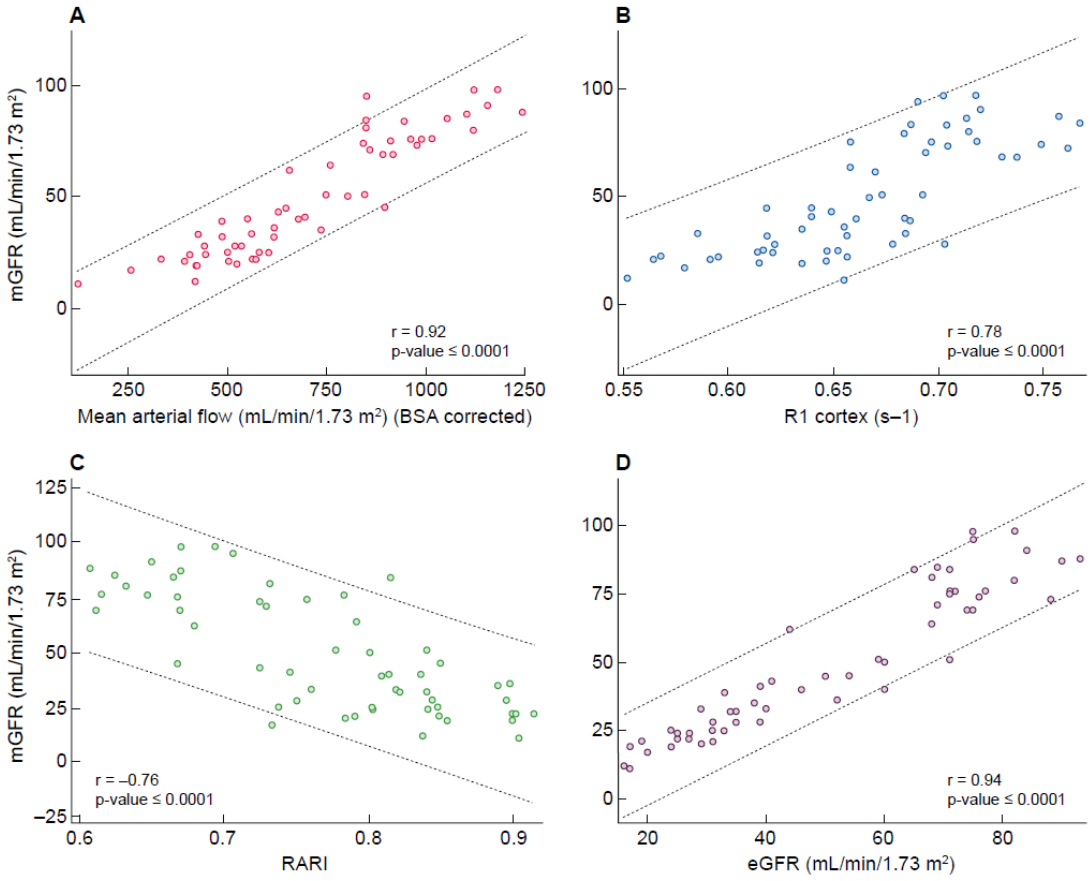

Figure 7: Scatter plots for mGFR versus MRI measures: A) MAF, B) Cortical R_1, C) RARI, and D) eGFR. Where: eGFR estimated Glomerular Filtration Rate; MAF = Mean Arterial Flow; mGFR = measured Glomerular Filtration Rate; MRI = Magnetic Resonance Imaging; RARI = Renal Arterial Resistive Index.